

设计指南: TIDA-010073

具有失速检测和速度控制功能的 18V、2A、25mm 有刷直流电机驱动器参考设计



说明

本参考设计展示了适用于扫地机器人主轮和主刷的有刷直流 (BDC) 电机驱动器解决方案, 无需任何其他传感器即可完成电机失速检测。本设计减少了组件数量, 具有小外形尺寸, 同时提供 BDC 电机控制的灵活性。本设计包含过流保护、过压保护、欠压保护和热关断等增强的保护功能。

资源

TIDA-010073	设计文件夹
DRV8876	产品文件夹
MSP430FR2111	产品文件夹
TPS709	产品文件夹

特性

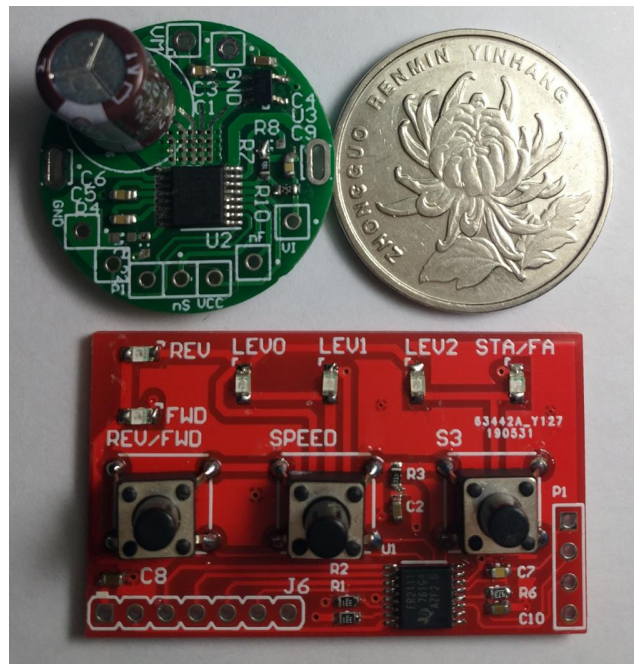
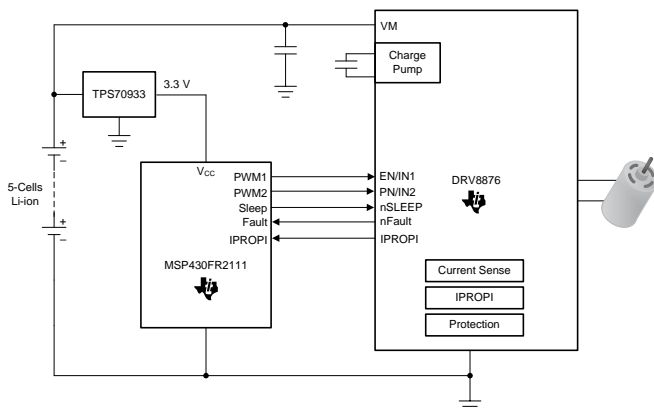
- 工作电压范围为 4.5V 至 33.6V
- 高输出峰值电流: 3.5A
- 具有集成式 H 桥前置驱动器和 FET
- 通过集成电流检测实现可靠的电机失速检测
- 具有过流、短路、过压、欠压和热保护功能。
- 工作环境温度: -40°C 至 85°C

应用

- 扫地机器人
- 无线真空吸尘器
- 冰箱和冷冻柜



咨询我们的 E2E™ 专家

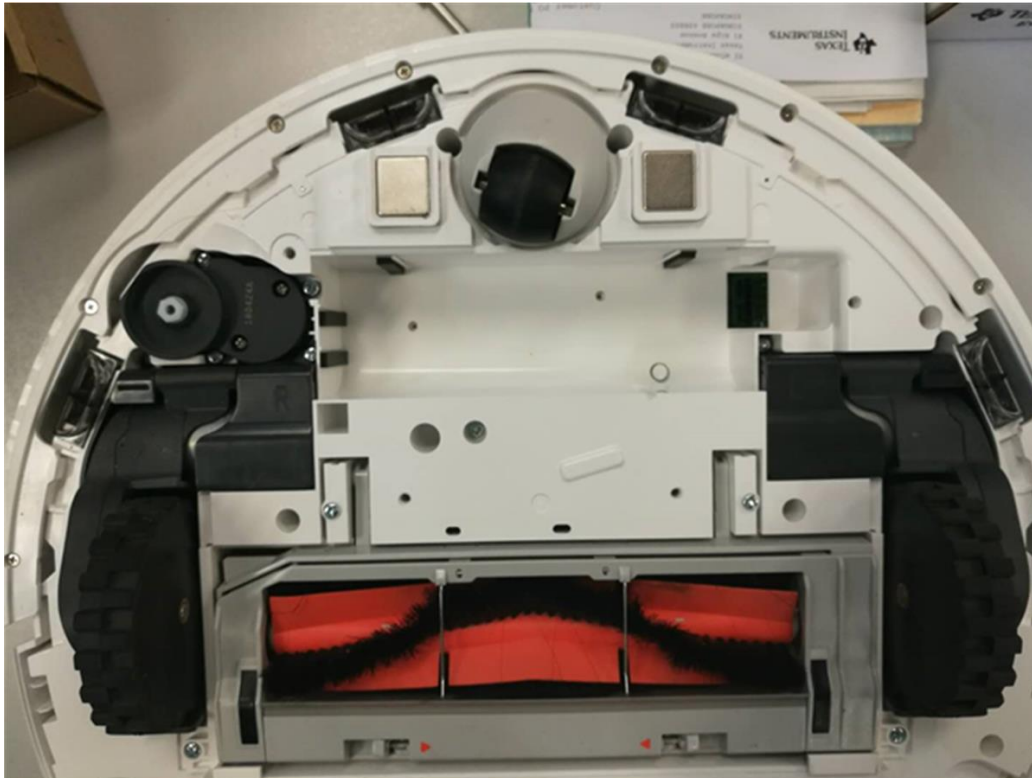


该 TI 参考设计末尾的重要声明表述了授权使用、知识产权问题和其他重要的免责声明和信息。

1 System Description

A robotic vacuum cleaner, often called a robovac or roboVac, is an autonomous robotic vacuum cleaner which has intelligent programming and a limited vacuum floor cleaning system. An advantage to using a *Robotic Vacuum Cleaner* (robovac) is that they vacuum automatically. Brushed DC motors are the popular choice because of the small body size. 图 1 shows a structure of a common robovac. The brushed DC motors are inside the main wheel and main brush.

图 1. Robovac Structure



The following list shows the general advantages of BDC motors:

- Small size
- Easy to drive
- Cost effective

1.1 Key System Specifications

表 1. Key System Specifications

PARAMETER	MIN	NOM	MAX	UNIT
DC input voltage ⁽¹⁾	4.5	18	33.6	V
Power level	0	-	30	W
Output current ⁽²⁾	0	2	3.5	A
Operation temperature	-40	25	85	°C
PCB Size	Control board: 25 mm × 42 mm Motor board: 25-mm diameter			

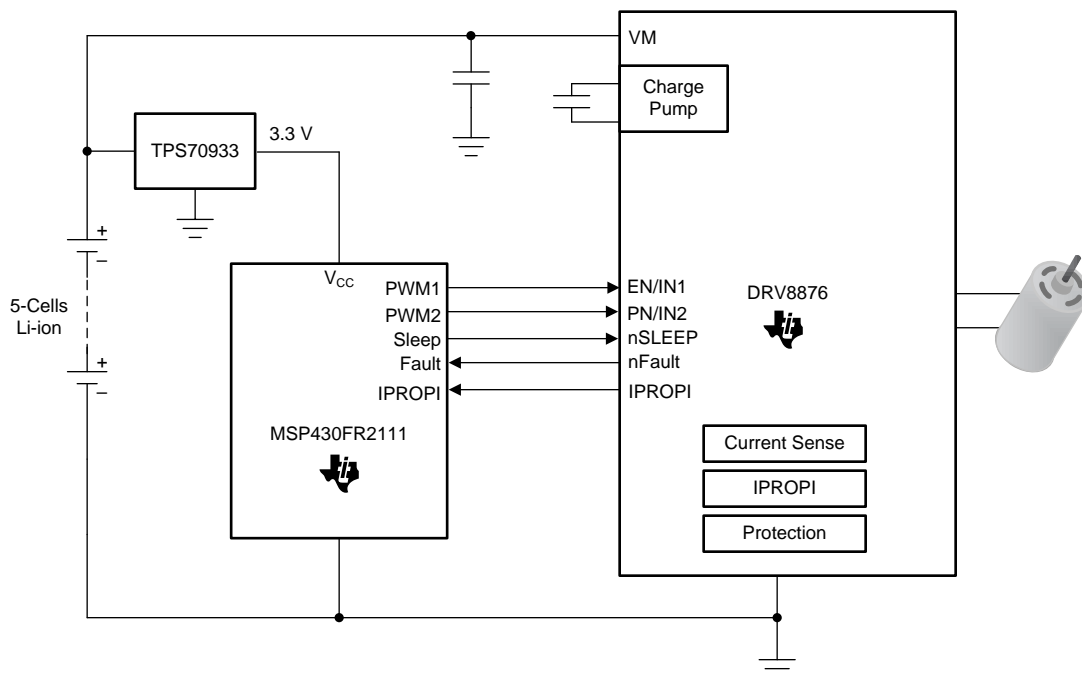
⁽¹⁾ This design can accept a 4.5-V to 35-V power supply, which fits the rated motor voltage. For this test setup, an 18-V nominal value (equal to a 5-cell Li-ion Battery) is used to run the specified motor.

⁽²⁾ Output current: 2 A for continuous output, 3.5 A for peak output.

2 System Overview

2.1 Block Diagram

图 2. TIDA-010073 Block Diagram



2.2 Design Considerations

This reference design is based on the TI DRV887x family of H-bridge drivers. The control MCU is TI's MSP430FR2111 which integrates the comparator and a 10-bit ADC.

The DRV887x family of devices are flexible motor drivers for a wide variety of end applications. The devices integrate an N-channel H-bridge, charge pump regulator, current sensing and regulation, current proportional output, and protection circuitry. The charge pump improves efficiency by allowing for both high-side and low-side N-channels MOSFETs and 100% duty cycle support. The family of devices come in pin-to-pin, scalable $R_{DS(on)}$ options to support different loads with minimal design changes. The MSP430FR21xx MCUs feature a powerful 16-bit RISC CPU, 16-bit registers, and a constant generator that contributes to maximum code efficiency.

2.3 Highlighted Products

The following subsections detail the highlighted products used in this reference design, including the key features for their selection. See their respective product data sheets for complete details on any highlighted device.

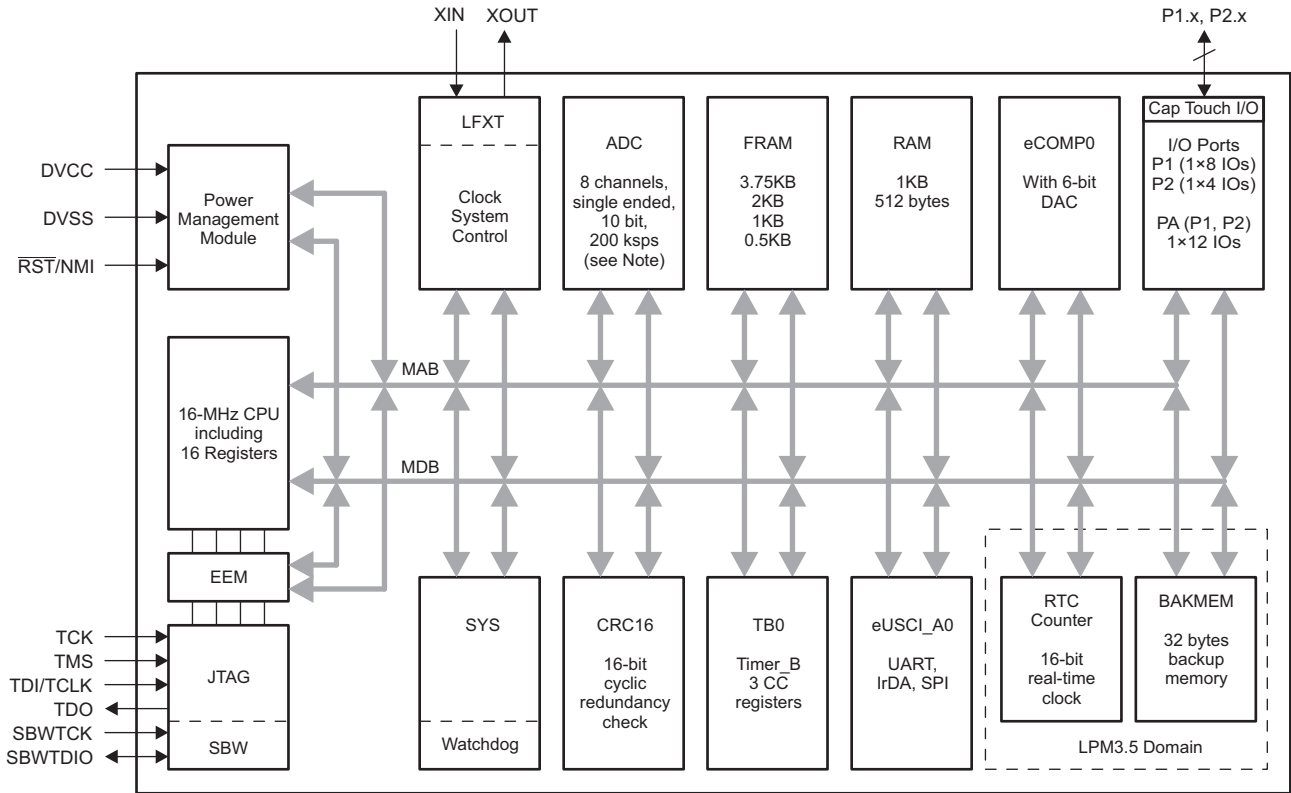
2.3.1 MSP430FR2111

The MSP430FR2111 devices are part of the MSP430™ microcontroller (MCU) value line sensing portfolio. This ultra-low power, low-cost MCU offers memory sizes 4KB of FRAM unified memory with several package options including a small 3-mm × 3-mm VQFN package. The architecture, FRAM, and integrated peripherals, combined with extensive low-power modes, are optimized to achieve extended battery life in battery-powered applications.

The MSP430FR2111 MCU features a powerful 16-bit RISC CPU, 16-bit registers, and a constant generator that contributes to maximum code efficiency. The digitally controlled oscillator (DCO) allows the device to wake up from low-power modes to active mode typically in less than 10 μ s.

The MSP430 ultra-low power (ULP) FRAM microcontroller platform combines uniquely embedded FRAM and a holistic ultra-low-power system architecture, allowing system designers to increase performance while lowering energy consumption. FRAM technology combines the low-energy fast writes, flexibility, and endurance of RAM with the nonvolatile behavior of flash.

图 3. MSP430FR2111 Functional Block Diagram



2.3.2 DRV8876

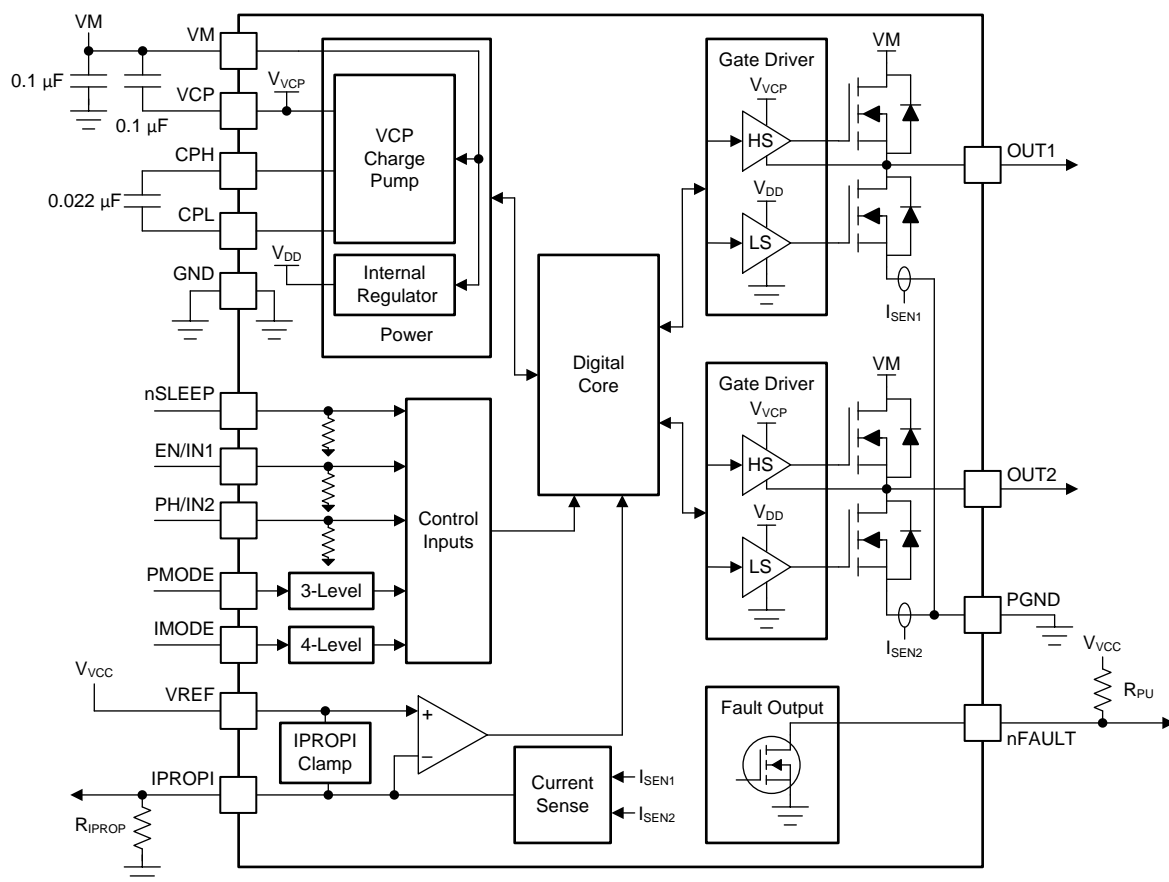
The DRV887x family of devices are flexible motor drivers for a wide variety of end applications. The devices integrate an N-channel H-bridge, charge pump regulator, current sensing and regulation, current proportional output, and protection circuitry. The charge pump improves efficiency by allowing for both high-side and low-side N-channels MOSFETs and 100% duty cycle support. The family of devices come in pin-to-pin, scalable $R_{DS(on)}$ options to support different loads with minimal design changes.

Integrated current sensing allows for the driver to regulate the motor current during start up and high-load events. A current limit can be set with an adjustable external voltage reference. Additionally, the devices provide an output current proportional to the motor load current. This can be used to detect motor stall or a change in load conditions. The integrated current sensing uses an internal current mirror architecture, removing the need for a large power shunt resistor, saving board area and reducing system cost.

A low-power sleep mode is provided to achieve ultra-low quiescent current draw by shutting down most of the internal circuitry. Internal protection features are provided for supply undervoltage lockout (UVLO), charge pump undervoltage (CPUV), output overcurrent (OCP), and device overtemperature (TSD). Fault conditions are indicated on nFAULT.

图 4 shows the DRV8876 block diagram.

图 4. DRV8876 Block Diagram



2.3.3 TPS70933

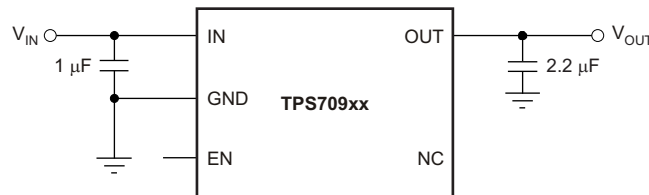
The TPS709 series of linear regulators are ultra-low, quiescent current devices designed for power-sensitive applications. A precision band-gap and error amplifier provides 2% accuracy over temperature. A quiescent current of only 1 μA makes these devices ideal solutions for battery-powered, always-on systems that require very little idle-state power dissipation. These devices have thermal-shutdown, current-limit, and reverse-current protections for added safety.

Shutdown mode is enabled by pulling the EN pin low. The shutdown current in this mode goes down to 150 nA, typical.

The TPS70933 device can be enabled as an optional choice in the reference design to evaluate the ultra-low standby power consumption.

图 5 shows the typical application circuit.

图 5. TPS70933 Typical Application Circuit



2.4 System Design Theory

For the BDC motor driver, usually the control is open-loop. The disadvantage of the simple control is obviously to be seen that the motor will be too hot to be damaged when the motor is blocked to stop. This design can show a solution that detects the motor stall condition without any other additional components. The internal comparator and ADC of MSP430FR2111 will help do the stall detection and motor speed calculation.

1. MSP430FR2111 – User interface, speed detection, and software based protection.
2. DRV8876 – H-bridge driver, current sensing and hardware protection
3. TPS709 – Ultra-low I_Q LDO

2.4.1 Motor Speed and Stall Detection

In many BDC electric motor applications, it is essential to keep track of the motor rotations to implement precise and reliable motion control. Traditionally this is done with optical sensors with photodiodes or Hall effect sensors both which pick up counting pulses from the rotating motor shaft or from the movements of the load attached to the motor shaft. These counting pulses are then sent back to the motor controller.

To reduce implementation complexity and cost in electric motor applications it is attractive to use sensor-less rotation counting methods, that is, methods where sensors and feedback wires with fragile connectors are not required.

2.4.2 Ripple Counting

Ripple Counting is a known sensor-less counting method. This method is based on measuring the fluctuations in the supply current to the motor as it rotates. Ripple Counting works on the 'law of induction', or more specifically Lenz's law, which says that the magnetic field of any induced current opposes the charge that induces it. This so-called Back Electromotive Force (BEMF) (sometimes called the counter electromotive force) can be detected by measuring the current flowing through each coil as the motor rotates.

The current measured in-line with the brushed motor has both a large-amplitude, very-low frequency DC component and a small-amplitude, high-frequency AC component. Both of these components must be considered when choosing the correct configuration for this design.

The total current seen in-line with the motor can be solved in [公式 1](#) as:

$$I_{motor} = \frac{(V_{ARMATURE} - V_{BEMF})}{R_{ARMATURE}}$$

where

- $V_{ARMATURE}$ is the DC voltage applied across the motor armatures
- V_{BEMF} is the BEMF generated by the motor during operation
- $R_{ARMATURE}$ is the equivalent series resistance seen between the armatures (1)

The DC-component current is the main source driving the inductive load of the motor. The motor load varies widely depending on the necessary torque to drive the mechanical motor assembly.

The AC-component current is created by the sinusoidal BEMF generated by the motor, as well as the periodic changes in motor coil impedance due to the motor brushes shorting adjacent commutator poles. The amplitude and frequency of this component also varies both on the mechanical load on the motor and the design of the motor itself. This AC component contains the ripple that the user should measure and is directly proportional to the actual motor speed. Every ripple corresponds to a commutator pole rotation across the armature brushes. The total sub-divisions of a full rotation can be captured by knowing the total number of poles in the motor.

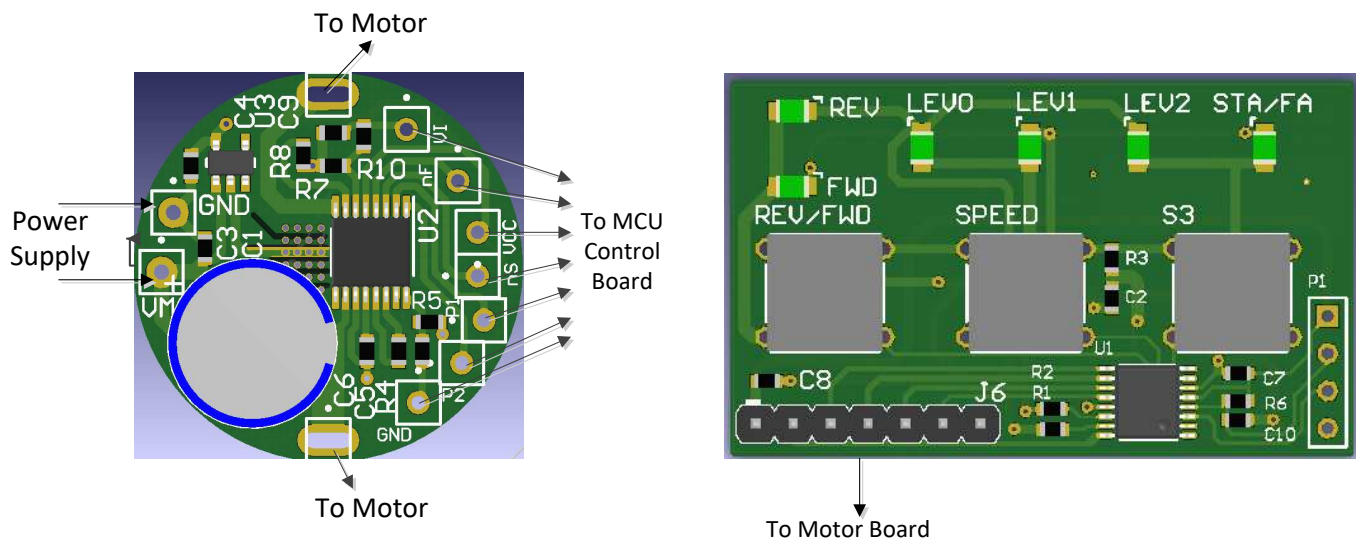
3 Hardware, Software, Testing Requirements, and Test Results

3.1 Required Hardware and Software

3.1.1 Hardware

图 6 shows the overview of the PCB for the TIDA-010073 design.

图 6. TIDA-010073 Printed-Circuit Board



The design includes 2 boards. The 20-mm diameter board is motor driver board which can be directly mounted on the back of the motor. The control board with LED and Key can set the motor speed, rotation detection and show the stall condition.

3.1.2 Software

Programming interface for MSP430 MCU

P1 is reserved as the programming interface for the MCU. The designer can program the MSP430 MCU using the JTAG port, Spy-Bi-Wire (SBW), and the bootloader BSL. In this reference design, SBW has been adopted for programming and is a two-wire SBW interface. Spy-Bi-Wire can be used to interface with MSP430 development tools and device programmers. 表 2 lists the SBW interface pin requirements. For further details on interfacing to development tools and device programmers, see the [MSP430 Hardware Tools User's Guide](#).

表 2. Spy-Bi-Wire Pin Requirements and Functions

PIN #	DEVICE SIGNAL	DIRECTION	SBW FUNCTION
1	PWM	-	Power supply
2	RST/SBWDIO	IN,OUT	SBW data input and output
3	TEST/SBWTCK	IN	SBW clock input
4	VSS	-	Ground

3.2 Testing and Results

3.2.1 Test Setup

表 3. Test Environment List

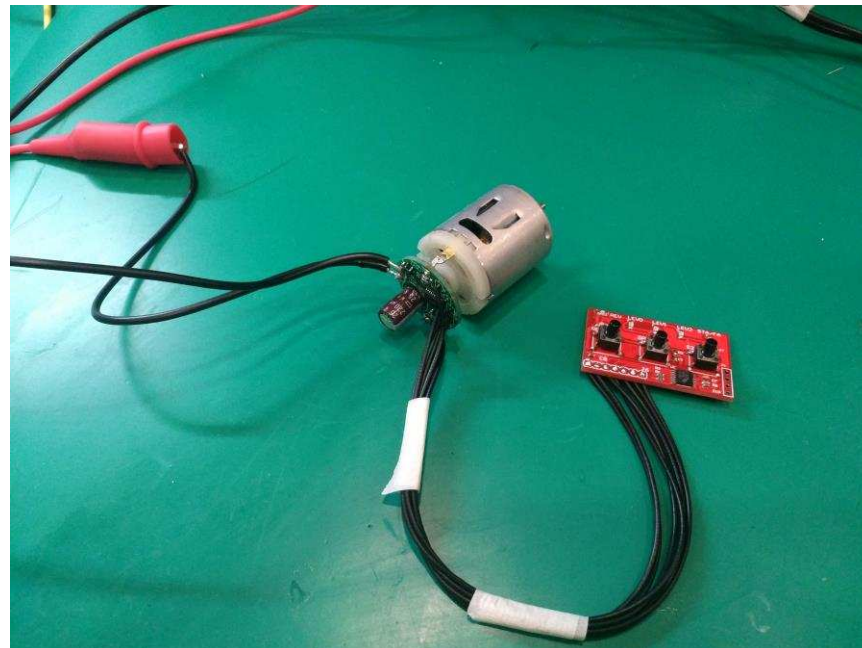
MATERIALS	USAGE	COMMENTS
MSP-FETFlash Emulation Tool	Debug and program	Emulation tool for MSP430FR2111
Computer	Debug and program	Code Composer Studio™ v8.2 installed PC with an USB port.
TIDA-010073 board	Main driver board and interface board.	With firmware programmed
BDC motor	Main motor	18-V, 2-A BDC motor for wheel.
DC Source	Power supply	30-V, 5-A Power source

The following steps show how to set up the test platform in the lab during the test:

1. Ensure that the firmware has been programmed into the MCU (see 节 3.1.2) in MCU board
2. Connect the motor with the 2 motor output pins. Any connection is available.
3. Connect the DC power source to the motor board. Keep the power OFF. Set the power output voltage between 16 V and 21 V. Set the current limitation up to 3.5 A.
4. Use the forward and reverse key to start the motor. Use the up and down key to control the motor speed.

图 7 shows the test setup in the lab, where the reference design is driving the BDC motor.

图 7. Test Setup With TIDA-010073 Reference Design



3.2.2 Test Results

The test results are listed in the following:

1. Current feedback from DRV8876

The DRV8876 integrates output current sensing using current mirrors on the low-side power MOSFETs. A proportional current is then sent out on the IPROPI pin and can be converted to a proportional voltage using an external resistor (RIPROPI).

图 8 和 图 9 show the current sense voltage at different loads. Channel 2 is the current probe. Channel 4 is the voltage probe by VIPROPI.

图 8. Current Sensing at High Load Condition

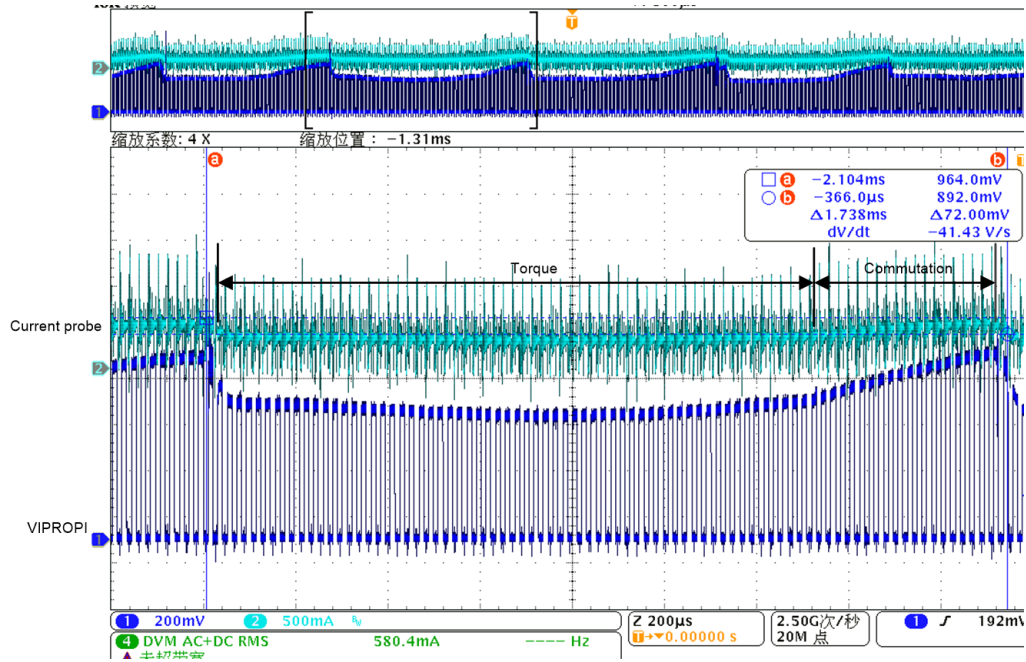
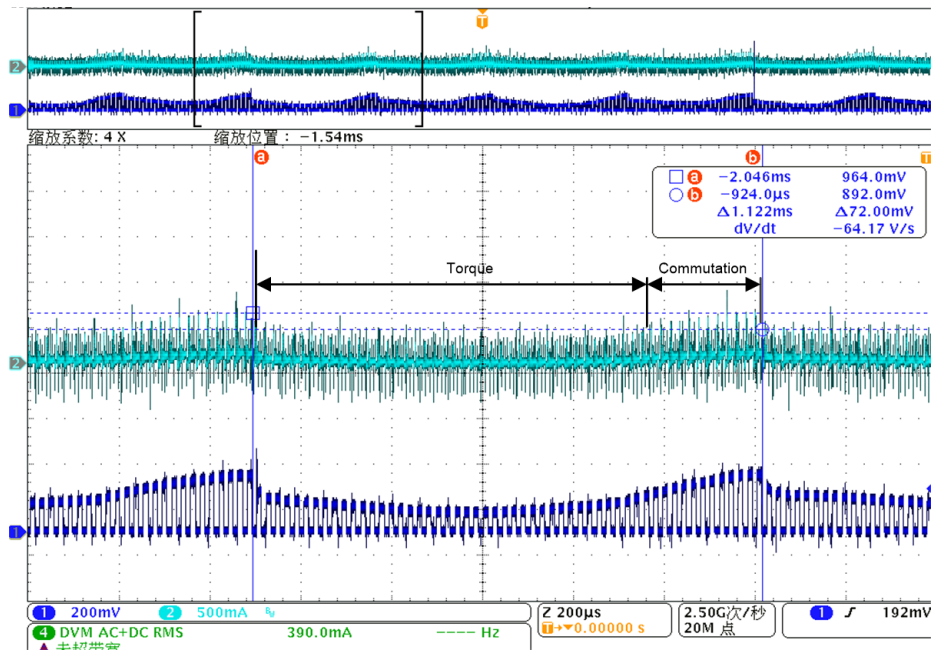


图 9. Current Sensing at Low Load Condition



2. Speed loop test result

The MCU software samples the phase current at each PWM on stage. The algorithm calculates the normal current based on the current at the torque stage and determines the commutation stage with the current ripple. The software also counts the speed between the 2 commutations.

表 4 shows the test results of the speed control:

表 4. Speed Control Test Results

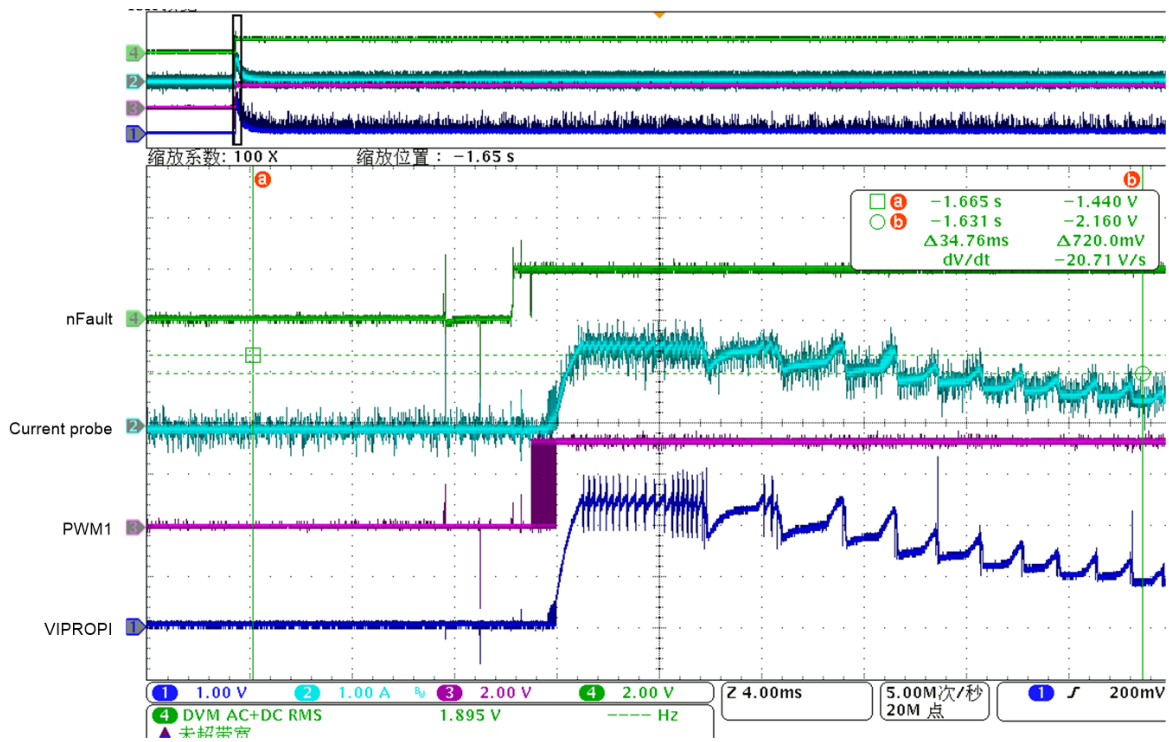
TARGET SPEED (RPM)	ACTUAL SPEED (RPM)	ERROR (%)
500	512	2.4
700	693	-1.0
900	908	0.9
1100	1089	-1.0
1300	1320	1.5
1500	1540	2.7
1700	1760	3.5
1900	1880	-1.1
2100	2069	-1.5
2300	2360	2.6
2500	2440	-2.4

The overall speed error can be controlled with 5% using the current ripple detection method.

3. Current limitation test result

Set the current limitation to 2.5 A. 图 10 shows the current limitation by hardware.

图 10. Current Limitation Test

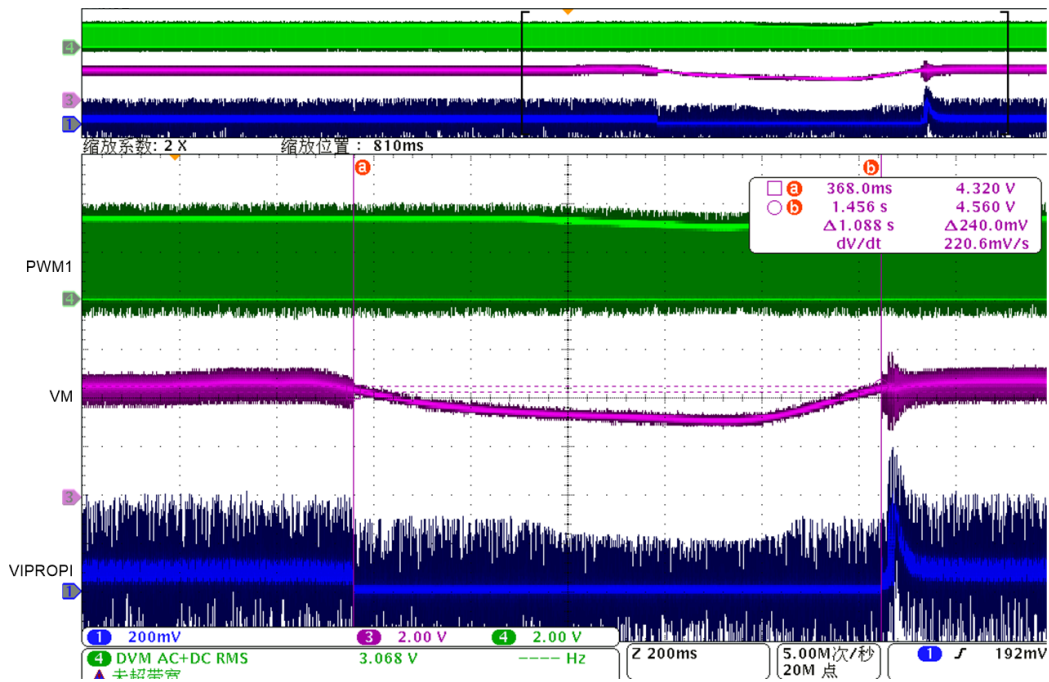


4. Protection test result

– Undervoltage lockout

The DRV8876 device monitors the VM voltage at any time. If the falling voltage is less than 4.35 V, it stops the output and generates an undervoltage protection. The protection is active until the voltage rises higher than 4.45 V, only then can it return to normal operation. 图 11 shows the undervoltage protection.

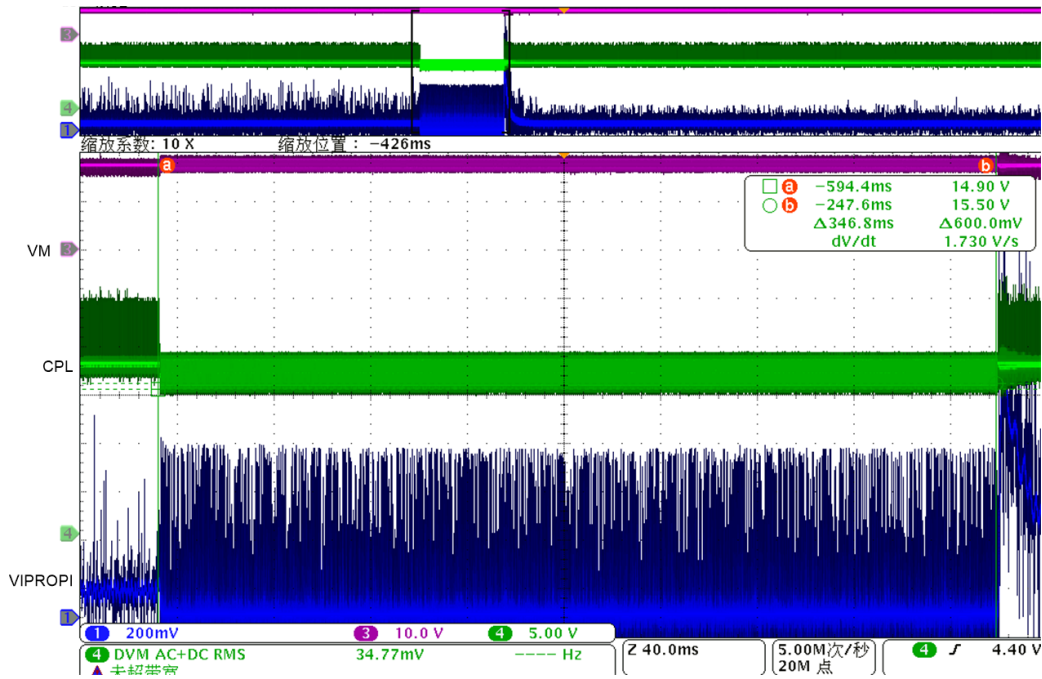
图 11. VM Undervoltage Protection



– Charge-pump undervoltage lockout

The DRV8876 device monitors the charge-pump voltage. If the charge pump voltage drops to 2.25 V, the hardware stops the output and generates a fault signal. After the charge-pump voltage is returned, the output can be recovered. 图 12 shows the charge-pump protection.

图 12. Charge-Pump Protection

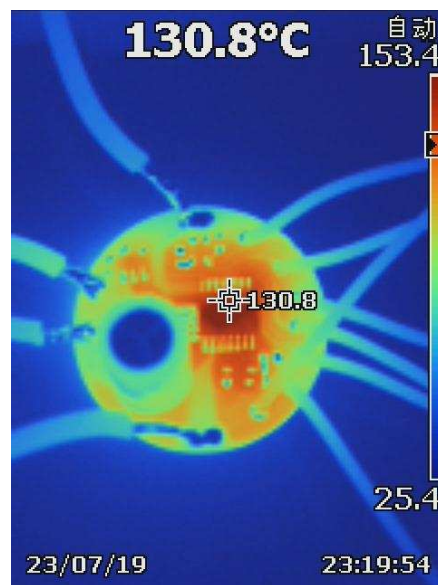


5. Thermal test

To better understand the temperature of power components and the maximum possible operating temperature, the thermal images were plotted at room temperature (25°C) with a closed enclosure and at 100% duty output conditions.

图 12 shows the thermal image for the top side of the board. The board is placed in a wide space without airflow.

图 13. Thermal Image



4 Design Files

4.1 Schematics

To download the schematics, see the design files at [TIDA-010073](#).

4.2 Bill of Materials

To download the bill of materials (BOM), see the design files at [TIDA-010073](#).

4.3 PCB Layout Recommendations

4.3.1 Layout Prints

To download the layer plots, see the design files at [TIDA-010073](#).

4.4 Altium Project

To download the Altium Designer® project files, see the design files at [TIDA-010073](#).

4.5 Gerber Files

To download the Gerber files, see the design files at [TIDA-010073](#).

4.6 Assembly Drawings

To download the assembly drawings, see the design files at [TIDA-010073](#).

5 Software Files

To download the software files, see the design files at [TIDA-010073](#).

6 Related Documentation

1. Texas Instruments, [MSP430FR21xx, MSP430FR2000 Mixed-Signal Microcontrollers Data Sheet](#)
2. Texas Instruments, [MSP430 Hardware Tools User's Guide](#)
3. Texas Instruments, [DRV8876 H-Bridge Motor Driver With Integrated Current Sense and Regulation Data Sheet](#)
4. Texas Instruments, [TPS709 150-mA, 30-V, 1- \$\mu\$ A IQ Voltage Regulators with Enable Data Sheet](#)

6.1 商标

E2E, MSP430, Code Composer Studio are trademarks of Texas Instruments.
Altium Designer is a registered trademark of Altium LLC or its affiliated companies.
All other trademarks are the property of their respective owners.

6.2 Third-Party Products Disclaimer

TI'S PUBLICATION OF INFORMATION REGARDING THIRD-PARTY PRODUCTS OR SERVICES DOES NOT CONSTITUTE AN ENDORSEMENT REGARDING THE SUITABILITY OF SUCH PRODUCTS OR SERVICES OR A WARRANTY, REPRESENTATION OR ENDORSEMENT OF SUCH PRODUCTS OR SERVICES, EITHER ALONE OR IN COMBINATION WITH ANY TI PRODUCT OR SERVICE.

7 About the Author

Fan (Hawken) Li is a systems engineer at Texas Instruments, where he is responsible for developing reference design solutions for the industrial segment. Hawken brings to this role his extensive experience in home appliances, including motor driver, EP, analog circuit design, and so forth.

重要声明和免责声明

TI“按原样”提供技术和可靠性数据（包括数据表）、设计资源（包括参考设计）、应用或其他设计建议、网络工具、安全信息和其他资源，不保证没有瑕疵且不做任何明示或暗示的担保，包括但不限于对适销性、某特定用途方面的适用性或不侵犯任何第三方知识产权的暗示担保。

这些资源可供使用 TI 产品进行设计的熟练开发人员使用。您将自行承担以下全部责任：(1) 针对您的应用选择合适的 TI 产品，(2) 设计、验证并测试您的应用，(3) 确保您的应用满足相应标准以及任何其他功能安全、信息安全、监管或其他要求。

这些资源如有变更，恕不另行通知。TI 授权您仅可将这些资源用于研发本资源所述的 TI 产品的应用。严禁对这些资源进行其他复制或展示。您无权使用任何其他 TI 知识产权或任何第三方知识产权。您应全额赔偿因在这些资源的使用中对 TI 及其代表造成的任何索赔、损害、成本、损失和债务，TI 对此概不负责。

TI 提供的产品受 [TI 的销售条款](#) 或 [ti.com](#) 上其他适用条款/TI 产品随附的其他适用条款的约束。TI 提供这些资源并不会扩展或以其他方式更改 TI 针对 TI 产品发布的适用的担保或担保免责声明。

TI 反对并拒绝您可能提出的任何其他或不同的条款。

邮寄地址：Texas Instruments, Post Office Box 655303, Dallas, Texas 75265

Copyright © 2022，德州仪器 (TI) 公司